1-1-1996

A Group of Galaxies at Redshift 2.38

Paul J. Francis
University of Melbourne

Bruce E. Woodgate
Association of Universities for Research in Astronomy, Inc. (AURA)

Stephen J. Warren
NASA Goddard Space Flight Center

Palle Møller
Imperial College London

Margaret Mazzolini
Space Telescope Science Institute

See next page for additional authors

Recommended Citation

Francis, Paul J.; Woodgate, Bruce E.; Warren, Stephen J.; Møller, Palle; Mazzolini, Margaret; Bunker, Andrew J.; Lowenthal, James D.; Williams, Ted B.; Minezaki, Takeo; Kobayashi, Yukiyasu; and Yoshii, Yuzuru, "A Group of Galaxies at Redshift 2.38" (1996). Astronomy: Faculty Publications, Smith College, Northampton, MA.
https://scholarworks.smith.edu/ast_facpubs/54

Authors

Paul J. Francis, Bruce E. Woodgate, Stephen J. Warren, Palle Møller, Margaret Mazzolini, Andrew J. Bunker, James D. Lowenthal, Ted B. Williams, Takeo Minezaki, Yukiyasu Kobayashi, and Yuzuru Yoshii

A Group of Galaxies at Redshift 2.38[1]

Accepted for Publication in Astrophysical Journal: To Appear Feb 1st 1996.

Paul J. Francis[2]
University of Melbourne, School of Physics, Parkville, Victoria 3052, Australia. e-mail: pjf@physics.unimelb.edu.au
Bruce E. Woodgate[2]
NASA Goddard Space-Flight Center, Code 681, Greenbelt, MD 20771. e-mail: woodgate@uit.dnet.nasa.gov
Stephen J. Warren
Imperial College, Astrophysics Group, Blackett Laboratory, Prince Consort Road, London SW7 2BZ, UK. e-mail: s.j.warren@ic.ac.uk
Palle Møller
Space Telescope Science Institute, Baltimore MD 21218, on assignment from the Space Science Department of ESA. e-mail: moller@stsci.edu
Margaret Mazzolini
University of Melbourne, School of Physics, Parkville, Victoria 3052, Australia. e-mail: marg@physics.unimelb.edu.au
Andrew J. Bunker
University of Oxford, Department of Physics, Keble Road, Oxford OX1 3RH, UK. e-mail: a.bunker1@physics.oxford.ac.uk
James D. Lowenthal[3]
Lick Observatory, Santa Cruz CA 95064. e-mail: james@lick.ucsc.edu
Ted B. Williams
Rutgers University, Physics and Astronomy Department, P. O. Box 849, Piscataway, NJ 08855-0849. e-mail: williams@fenway.rutgers.edu
Takeo Minezaki
Department of Astronomy, Faculty of Science, University of Tokyo, Bunkyo-ku, Tokyo 113, Japan. e-mail: umineza@c1.mtk.nao.ac.jp
Yukiyasu Kobayashi
National Astronomical Observatory, Mitaka, Tokyo 181, Japan. e-mail: yuki@merope.mtk.nao.ac.jp
&
Yuzuru Yoshii

Institute of Astronomy, University of Tokyo, Mitaka, Tokyo 181, Japan.
e-mail: yoshii@omega.mtk.ioa.s.u-tokyo.ac.jp

[1] Based on observations collected at Cerro Tololo Interamerican Observatory, the European Southern Observatory (La Silla, Chile), Siding Spring Observatory, the Australia Telescope, and the Anglo-Australian Observatory

[2] Visiting Astronomer, Cerro Tololo Interamerican Observatory. CTIO is operated by AURA, Inc. under contract to the National Science Foundation.

[3] Hubble Fellow

Abstract

We report the discovery of a group of galaxies at redshift 2.38. We imaged $\sim 10\%$ of a claimed supercluster of QSO absorption-lines at $z = 2.38$ (Francis & Hewett 1993). In this small field ($2'$ radius) we detect two Ly-α emitting galaxies. The discovery of two such galaxies in our tiny field supports Francis & Hewett's interpretation of the absorption-line supercluster as a high redshift 'Great Wall'.

One of the Ly-α galaxies lies $22''$ from a background QSO, and may be associated with a multi-component Ly-α absorption complex seen in the QSO spectrum. This galaxy has an extended ($\sim$ 50kpc) lumpy Ly-α morphology, surrounding a compact IR-bright nucleus. The nucleus shows a pronounced break in its optical-UV colors at $\sim$ 4000Å (rest-frame), consistent with a stellar population of mass $\sim 7 \times 10^{11}\mathrm{M}_{\mathrm{Sun}}$, an age of $>$ 500Myr, and little on-going star-formation. C IV emission is detected, suggesting that a concealed AGN is present. The Ly-α emission is redshifted by $\sim$ 490km s^{-1} with respect to the C IV emission, probably due to absorption. Extended H-α emission is also detected; the ratio of Ly-α flux to H-α is abnormally low (~ 0.7), probable evidence for extended dust.

This galaxy is surrounded by a number of very red ($B - K > 5$) objects, some of which have colors suggesting that they too are at $z = 2.38$. We hypothesize that this galaxy, its neighbors and a surrounding lumpy gas cloud may be a giant elliptical galaxy in the act of bottom-up formation.

Note: The figures for this paper are available in this archive, by anonymous FTP to tauon.ph.unimelb.edu.au in the directory /incoming/pjf/paper, or on the WWW from

`http://www.ph.unimelb.edu.au/~pjf/blob.html`

1 Introduction

The extent of galaxy clustering at high redshifts ($z > 1$) is controversial. CDM and similar models predict that most large-scale structure forms at redshifts below one. This is consistent with the rapid evolution in galaxy clusters seen between $z \sim 0.5$ and the present (Butcher & Oemler 1978, Edge et al. 1990). Further evidence comes from the apparently weak clustering of faint blue galaxies at $z \sim 0.7$ (Efstathiou et al. 1991) and the weak clustering of Ly-α forest clouds (eg. Carswell & Rees 1987).

On the other hand, an increasing body of data suggests that galaxies at redshifts above one are strongly clustered on large scales. Evidence comes from metal-line QSO absorption systems (eg. Heisler, Hogan & White 1989, Jakobsen & Perryman 1992, Foltz et al. 1993, Møller 1995, Williger et al. 1995), from the association of Ly-α emitting galaxies with damped Ly-α absorption systems and QSOs (Wolfe 1993, Djorgovski et al. 1985), and from the often serendipitous discovery of individual clusters (eg. Dressler et al. 1993, and possibly Giavalisco, Steidel & Szalay 1994).

Francis & Hewett (1993) claim to have discovered two coherent structures of gas, at least ten co-moving Mpc in size, one at redshift 2.38, the other at 2.85. These postulated structures cause Ly-α absorption at matching redshifts in the spectra of two background QSOs separated by $8'$. The authors discuss two possibilities: either the gas structures are primordial pancakes, or 'Great-Wall' style galaxy superclusters. In both cases, these structures would be the most dramatic examples yet of large scale structure at high redshift.

In this paper, we attempt to confirm the existence of one of Francis & Hewett's enormous structures. We have studied a small part of the postulated z=2.38 structure, using a wide range of optical, infra-red and radio observations on ten different southern hemisphere telescopes (§ 2). Our initial aim was to search for Ly-α emitting sources at this redshift, using narrow-band Fabry-Perot imaging. We found at least two Ly-α emitting galaxies at z=2.38 (§ 3.1) one of which has a remarkable extended Ly-α morphology. Extensive follow-up observations at many frequencies revealed a number of other possible galaxies at z=2.38.

We describe our observations in § 2, results are shown in § 3, and discussed in § 4. Throughout this paper, we will assume that $H_0 = 75$ km s^{-1}Mpc^{-1} and $q_0 = 0.5$.

2 Observations

Due to limited observing time and poor weather, we were able to observe only a small part of one of Francis & Hewett's postulated structures. We chose to study the $z = 2.38$ structure, and imaged the field around one of the two background QSOs, 2139-4434. The absorption line system in 2139-4434 at $z = 2.38$ consists of at least three components, a central one of wavelength 4108.5Å and neutral hydrogen column density $\sim 7 \times 10^{18}$cm^{-2}, and two lower column density systems (Fig 4). Given the limited resolution of our spectra, we have not attempted a decomposition of the two subsidiary absorption systems, but we estimate their wavelengths as being 4101Å and 4119 Å. All three may well be blends of lower column-density lines.

2.1 Optical Imaging

The first step in our imaging campaign was to search for redshifted Ly-α emission from galaxies at $z = 2.38$. A field surrounding the QSO 2139-4434 was imaged on the nights of 1994 June 4th and June 5th, using the Rutgers Fabry-Perot system (Gebhardt et al. 1994) with Goddard etalons, on the CTIO 4-m telescope. The etalon was set to a central wavelength of 4110 Å with a width of 30 Å. The relatively large width was chosen to allow for possible peculiar velocities relative to the main absorption system, as suggested by the wavelengths of the subsidiary absorption systems. We alternated 1800 second exposures on-band with 360 second exposures off-band. Off-band exposures were also taken through the etalon, but with the plate spacing altered to shift the central wavelength away from the absorption line wavelength, and with the order-blocking filter removed. This increased the count rate from continuum sources by a factor of ~ 5. The similarity of the set-up between on- and off-band exposures was intended to prevent any ghost images showing up as narrow-band excess objects. The telescope was offset by $\sim 5''$ in a random direction between pairs of on- and off-band exposures to improve flat fielding and as an additional precaution against ghosts.

Six pairs of on- and off-band images were taken on each night (Fig 1). Seeing was $\sim 1.6''$ (Full Width at Half Maximum Height, FWHM) throughout. Images taken on the first night suffered from poor throughput in the order-blocking filter; a more efficient filter was used on the second night. A narrow-band flux limit of 8.4×10^{-17} erg cm^{-2} s^{-1} for a point source was reached (3σ). All images were reduced using standard IRAF[1] procedures,

---

[1] IRAF is distributed by the National Optical Astronomy Observatories, which is operated by the Association of Universities for Research in Astronomy, Inc. (AURA) under

then shifted and added using inverse variance weighting to maximize the final signal-to-noise ratio. Due to light cirrus during the observations, only relative photometry was obtained, bootstrapped from CCD-calibrated UK Schmidt plate scans. This introduces an uncertainty of ~ 0.15 magnitudes in the photometry.

Candidate narrow-band excess objects were selected in a variety of ways. On- and off-band images were blinked and compared by eye, and both aperture photometry and DAOPHOT were used. All approaches were cross checked and found to give consistent answers. Automatic procedures needed substantial human intervention, due to the strong signal-to-noise gradient across the frames caused by the shifting and adding, which principally manifested itself in spurious sources near the edge of the field. All fluxes quoted in the paper are total fluxes. For fainter unresolved objects, photometry was carried out using a small aperture (diameter $\sim 1.6''$, the seeing FWHM) and corrected up to a total flux using the PSF of bright isolated stars in the field. Flux and magnitude limits are quoted for the area around QSO 2139$-$4434 where the noise is a minimum, and for an aperture of diameter $\sim 1.6''$.

An additional *B*-band image was obtained on the CTIO 0.9-m using the Tek 2k chip, giving a $12' \times 12'$ field centered on a point mid-way between the two background QSOs and including the fields around both QSOs. A total of 10800 seconds exposure was obtained on the night of 1994 June 7th.

I and *B* band images of the field around 2139-4434 were obtained on the night of 1994 August 5th with the EFOSC camera (Eckert, Hofstadt & Melnick 1989) on the ESO 3.6-m telescope. Exposure times were 2700 s in *B* and 1620 s in *I*, and the seeing was poor ($\sim 2.5''$). The *I*-band image reached a limiting magnitude of 23 (3σ). A weighted sum of the two *B*-band images reached a limiting magnitude of 24.7 (3σ). Photometry of these frames was carried out as above.

Astrometry for all frames was bootstrapped from positions in the COSMOS database, maintained on-line at the Anglo-Australian Observatory. In each image, 5 stars were used to obtain a 6-coefficient plate solution. Residuals from the fit (rms) in each coordinate were $0.15''$ for the CTIO 4-m images, $0.12''$ for the ESO 3.6-m images, and $0.12''$ for the Siding Spring 2.3-m IR-images.

---

cooperative agreement with the National Science Foundation.

2.2 IR Imaging

IR imaging was obtained on the nights of 1994 September 25th to September 28th on the Siding Spring Observatory 2.3-m telescope, using the PICNIC near-IR camera (Kobayashi et al. 1994). The detector field-of-view was centered midway between the QSO and galaxy B1 (see § 3.1). PICNIC has a 256×256 NICMOS chip, with $0.5''$ pixels. 250 exposures, each of 17 seconds, were obtained in both H and K' bands, rastered on a 5×5 grid, in $1.0''$ seeing. Limiting magnitudes were 21.0 in both H and K' ($3\ \sigma$). 75 exposures, each of 67 seconds, were taken through an interference filter, of central wavelength 2.238 μm and width (FWHM) 0.048 μm, roughly matching the expected wavelength of H-α emission at $z = 2.38$. The K' image was used as the off-band for this H-α image, and a (3σ) flux limit of 4.5×10^{-16} ergs cm^{-2} s^{-1} was reached. Conditions were photometric, accuracy being limited by a slight time-dependence in the flat field to ~ 0.1 magnitudes.

Further IR imaging was obtained with the IRAC-2B camera on the ESO/MPI 2.2-m. 22 exposures of 300 seconds were taken centered on the QSO in the J band, in non-photometric conditions on 1994 Oct 25th. Photometric calibration was obtained from 5 exposures of 180 seconds each taken on 1994 November 18th, with the same instrument. Seeing was $1.1''$ and the 3σ magnitude limit is 21.77. 29 exposures of 300 seconds were also taken in K' in photometric conditions on 1994 Oct 24th.

2.3 Spectroscopy

We detected three possible Ly-α emitting galaxies in our narrow-band imaging, B1, B2 and B3 (see § 3.1 below). Follow-up spectroscopy of two of these candidates, B1 and B2, was obtained on the nights of 1994 Aug 4th and 5th with the EMMI instrument (Dekker et al. 1991) on the NTT. The slit was placed over the background QSO at such an angle that it would also cover the galaxy candidate. In the case of B1, the slit passed through the peak narrow-band emission, but $2''$ south-west of the IR-bright nucleus. Blue arm spectra of both objects were taken with BLMD, with the # 3 grism and a $2''$ slit giving a resolution of 2.35Å. Exposure times were 7200 seconds for both candidates. In addition, a red arm spectrum of B1 was taken with RILD, grating # 5, a $1.5''$ slit and an exposure time of 4800 seconds, the resolution being $\sim$ 7Å.

Additional spectra of B1 were taken at the AAT on September 6th 1994. The slit was laid along the major axis of B1 and 9000 seconds integration obtained. Seeing was $\sim 4''$, preventing us from obtaining any useful spatial information. The RGO spectrograph, with the 600V grating set blaze to collimator, and the faint object red spectrograph, were used simultaneously, with the dichroic.

2.4 Radio Observations

The field containing all the galaxy candidates was observed with the Compact Array of the Australia Telescope on Jan 26th and Jan 28th 1995. A total of 20 hours of observations were obtained both at 1344 and 2378 MHz, with the 6A configuration. The data were reduced using standard procedures embodied in the MIRIAD package, and CLEANed with a restoring beam of 6.8×4.7 arcsec at 1344 MHz and 3.8×2.5 arcsec at 2378 MHz. The field has also been surveyed at 847 MHz with the Molonglo Synthesis Telescope (Hunstead, private communication). Although radio-quiet, QSO 2139-4434 is detected at all three frequencies, with fluxes of 3.8 ± 1.1 mJy at 847 MHz, 1.61 ± 0.09 mJy at 1344 MHz and 0.86 ± 0.09 mJy at 2378 MHz. Nothing else is detected in the field at any wavelength, 3σ limits being 3.3 mJy (847 MHz) and 0.27 mJy (1344 and 2378 MHz).

3 Results

3.1 Line-Emitting Galaxies

We detected three candidate Ly-α emitting galaxies, B1, B2 and B3 (Fig 1, Fig 2). All three were seen in the narrow-band Ly-α image, but not in the off-band Fabry-Perot image, though B3 is only detected with $\sim 2.7\sigma$ confidence. Our spectra of B1 and B2 show that the narrow-band image flux is indeed due to a strong isolated emission-line. For B1 we also detect C IV and H-α emission, confirming the identification of the line as Lyman-α. The properties of these candidates are shown in Table 1.

Object B1 lies $22''$ from the background QSO, and has an extended emission-line morphology (Fig 3). A knot of Ly-α flux lies at the Southwest of B1, marginally resolved (FWHM $\sim 4''$, 18kpc) and contributing roughly half the flux. The remainder comes from a tail extending $\sim 10''$ (50 kpc) to the North-East.

Object B1 has an H-α flux of $(9.2 \pm 1.5) \times 10^{-16}$ erg cm^{-2} s^{-1} (1σ errors). The H-α emission morphology is similar to that of the Ly-α morphology. Note that H-α contributes less than 10% of the K'-band flux. C IV is detected with 3σ confidence, at a position on the slit corresponding to the peak of the Ly-α emission. The ratio of Ly-α to C IV is $\sim$ 7:1 at this position. A possible He II line is seen at $\sim 2\sigma$ confidence, about 50% weaker than C IV; no other significant emission features are seen.

The redshift of B1, as deduced from the C IV emission (Fig 5), is 2.3796, identical within the errors ($\sim$ 100 km s^{-1}) to that of the centroid of the QSO absorption-line (Fig 5). However, the Ly-α emission is redshifted by $\sim$ 490 km s^{-1} with respect to both of these lines. The Ly-α line is strongly red asymmetric, and has a velocity width of $\sim$ 600 km s^{-1}. The apparent relative displacement of Ly-α and C IV may be caused by Ly-α absorption (§ 4.2).

B1 is not seen in any of the broad-band optical images. No continuum is seen in the blue spectra, though a faint continuum is seen with about 2σ confidence in the red spectrum, giving B1 a tentative continuum magnitude of 25.8 at 5000 Å. In the near-IR however, a strong unresolved source is seen, lying within the extended Ly-α morphology. This source is marginally detected in the J band ($J \sim 22.0$) but is relatively bright in H and K' ($H = 19.9$, $K' = 19.0$).

The Ly-α knot and the IR source are misaligned by $\sim 2.5''$. This misalignment is real; the two images have internal astrometry accurate to $\sim 0.15''$. The colors of the IR source show a pronounced break at $\sim 1.3\mu$m, which is the expected position of the Balmer or 4000Å break at $z = 2.38$. Objects showing such a near-IR spectral break are rare; only four are seen in our 7800 square arcsec field of view. Given this surface density, the probability of such an object lying within $2.5''$ of the peak of the Ly-α emission is 0.2% . We therefore consider it highly probable that the IR source is at the same redshift as, and associated with, the Ly-α emission. H-α emission comes from the same region as Ly-α emission; the H-α emission is detected from both the Ly-α knot and tail with $> 4\sigma$ confidence, having approximately equal H-α fluxes. The H-α image also shows flux at the position of the continuum IR source, no more that would be expected from a featureless continuum spectrum. The signal-to-noise ratio of the H-α image is too poor to allow any other morphological information to be extracted.

Object B2 lies $63''$ from the background QSO, and is unresolved. It is marginally detected ($\sim 2\sigma$ confidence) in the K' image ($K' \sim 20.8$), and not detected in any other band. We only detect the one line in B2, but its equivalent width is much greater than that of [O II] in a typical field galaxy (Colless et al. 1990, Glazebrook et al. 1995), strongly suggesting that the line is indeed Ly-α at $z = 2.38$. H-α is not detected, the upper limit being 4.5×10^{-16} erg cm^{-2} s^{-1} (3σ). B2's Lyman-α emission is redshifted by 160 km s^{-1} with respect to the absorption-line centroid, has a red asymmetric profile, and a velocity width (FWHM) of ~ 450 km s^{-1}. No other lines are seen in the blue spectrum, the upper limit on their flux being 30% that of B2, but the spectrum only covers the rest-frame wavelength region 1182–1320 Å, so no other strong lines would be expected.

B3 is detected with only $\sim 2.7\sigma$ confidence; we have no color or spectral information on it.

3.2 Broad-band Colors

When we obtained IR images of our field, we were surprised to find that the QSO 2139-4434 and B1 are surrounded by a group of very red ($B - K' > 5$) objects, extending over $\sim 50''$ (Fig 6). Multicolor photometry gives us some clues to the redshifts of these objects.

B1 itself, as discussed above, shows a clear spectral break at about 1.3μm (Fig 7), which we ascribe to the redshifted Balmer or 4000Å break, giving it an $I - H$ color of 3.1. Most of the other red objects near it have $I - H < 2.5$; they have relatively flat spectral energy distributions between the I and K' bands, and very red $B - I$ colors. Spectral energy distributions of the two brightest of these objects are shown in Fig 7 as examples. These objects are unlikely to be associated with the Francis & Hewett supercluster; instead their colors are typical of galaxies at $0.3 < z < 1.2$.

A few of B1's red neighbors do have colors consistent with a redshifted Balmer or 4000Å break at $z \sim 2.38$. These candidate supercluster members are marked as squares in Fig 2, and their spectral energy distributions are shown in Fig 7. In most cases they are too faint to say with confidence whether they show a strong redshifted spectral break; further deep I-band photometry will resolve this question.

A number of other objects in the field of view but more distant from B1 also have large $I-K'$ colors, and hence are candidate $z = 2.38$ objects. These objects are marked as squares in Fig 2, and the spectral energy distributions of the two best candidates are shown in Fig 7.

Could any of these very red objects be M-dwarfs? Leggett (1992) showed that the optical/near-IR colors of M-dwarfs lie in a well defined subset of the color space. B1 and the other candidate $z = 2.38$ galaxies, however, show very different colors. In particular, their $J - K'$ colors are much redder than those of any of the dwarf stars studied by Leggett. We therefore consider it unlikely that these objects are galactic stars.

In conclusion, the very red objects surrounding the QSO and B1 fall into two classes; objects with spectral breaks between the B and I bands, which are probably foreground galaxies, and objects with spectral breaks between the I and H bands, which are probably at the same redshift as the QSO absorption lines, B1 and B2.

3.3 The QSO Sight-line

The line of sight to the background QSO, 2139−4434, lies $22''$ from B1. We performed a point spread function (PSF) subtraction on our images to look for a possible absorbing galaxy closer to the line of sight.

The PSF subtraction in the Ly-α and B-band images revealed nothing. The QSO is not black in the Ly-α image as our filter passband was wider than the absorption line. We would not detect objects within $\sim 1''$ of the QSO sight line.

In the I band and the IR images, a source is seen $1.8''$ from the QSO sightline, lying roughly 30° east of north. This source is most clearly seen in the K' image. This object has a flat spectral energy distribution between I and K' but is very red in $B - I$ ($B > 24$, $I \sim 20.4$, $K' \sim 18.3$). These colors are very similar to those of the candidate foreground galaxies discussed in § 3.2 above, and we therefore hypothesize that like them this object lies at a redshift $0.3 < z < 1.2$.

Note that the presence of so many intermediate redshift galaxies close to the QSO sight-line may not be coincidental; they may be gravitationally lensing QSO 2139-4434, amplifying it enough to bring it into the QSO sample (eg. Webster et al. 1988, Rodrigues-Williams & Hogan 1994).

4 Discussion

4.1 The Supercluster?

Francis & Hewett claim that their absorption-line supercluster has an overdensity of > 30 (95 % confidence), although they were unable to determine whether it was some sort of primordial pancake or a 'Great Wall' style supercluster.

Our detection of galaxies near one of the QSO absorption line clouds suggests that it is indeed a galaxy cluster and not a primordial pancake, though it may be a very gas rich supercluster. Following the argument of Wolfe (1993) we can estimate the overdensity of Ly-α emitting galaxies in the imaged field, by comparing our galaxy detections with the null results reported by field searches for Ly-α emission.

As our control sample, we will use the search for field Ly-α emitting galaxies carried out by Pritchet & Hartwick (1990). They claim to have searched a co-moving volume 100 times larger than ours, down to a limiting flux of 5.4×10^{-17} erg cm^{-2} s^{-1} arcsec^{-2} (2σ). B1 has a peak surface brightness of 1.6×10^{-16} erg cm^{-2} s^{-1} arcsec^{-2}. B2 is unresolved in $\sim 1.6''$ seeing; we measured a peak surface brightness of 9.6×10^{-17} erg cm^{-2} s^{-1} arcsec^{-2}. Both B1 and B2 thus easily exceed their quoted flux limit, unless their seeing was very poor. Pritchet & Hartwick do not explicitly state their equivalent width limit, but they imply that they were sensitive to objects showing > 0.1 magnitude differences between their on- and off-band images, implying an equivalent width limit $\ll 50$Å. Both B1 and B2 have equivalent widths much greater than this. It is therefore probable that if any objects such as B1 and B2 existed in the region surveyed by Pritchet & Hartwick, they would have been found.

We calculate limits on the overdensity of Ly-α galaxies in our field as follows. Firstly, we assume a background Ly-α galaxy density ρ and an overdensity of Ly-α galaxies in our field ω, defined as the ratio of the mean Ly-α galaxy density in our field divided by the background Ly-α galaxy density. Using Poisson statistics, we then derive the probability of seeing two or more galaxies in our field P_f, and the probability of seeing no galaxies in Pritchet & Hartwick's survey P_p. We then vary ρ to maximize the joint probability $P_j = P_f P_p$, for a given value of ω.

If our field is in no way special ($\omega = 1$), the peak joint probability is

5×10^{-5}. We can therefore reject the null hypothesis that Ly-α galaxies are not overdense in our field. For larger values of ω, the maximum joint probability increases, and occurs for smaller ρ. To bring P_j up to 5% , we require $\omega > 15$; our field must have an overdensity of a factor of at least 15 (95% confidence).

An overdensity of > 15 in our $2'$ radius field, while consistent with Francis & Hewett's claim, is not in itself very surprising; $2'$ corresponds to a proper distance scale of $\sim$ 500 kpc, and overdensities of > 15 on these scales are common in the local universe. If however the overdensity remains this high over the whole postulated supercluster, $> 8\,'$ in diameter, this would be surprising. The only object in the local universe approaching such overdensities on these large scales is the Great Wall. Heisler et al. (1989) and Wolfe (1993) argue that the existence of structures this large and dense at high redshifts is a challenge for gravitational structure formation models such as CDM. The location of B2, C1 and C2 near the edge of our field of view suggests that the galaxy overdensity does indeed continue beyond the field we have imaged to date.

The main weakness with this analysis is with the control sample. Pritchet & Hartwick's sample is at the slightly lower redshift of $z \sim 1.9$. If the number density of Ly-α galaxies was evolving strongly between $z = 2.38$ and $z \sim 1.9$ the overdensity in our field might be much lower. De Propris et al. (1993) carried out a field search for Ly-α emitting galaxies between redshifts 2–3 and discovered none, but unfortunately their survey was insufficiently deep to detect objects with fluxes comparable to B1 and B2. The many other unsuccessful Ly-α galaxy searches, many at redshifts above 2.38 (eg. Lowenthal et al. 1995, Djorgovski, Thompson & Smith 1993) however make us doubt that the numbers of Ly-α galaxies are evolving strongly. It is also worrying that Pritchet & Hartwick were selecting their candidates by eye; De Propris et al. (1993), using an almost identical technique, were only finding $\sim$ 50% of simulated 10σ galaxies. Clearly a quantitative analysis of deeper control fields at $z \sim 2.4$ would help.

Assuming that our analysis is valid, and that the overdensity of galaxies really does extend to Mpc scales, one possible explanation is that the distribution of Ly-α emitting galaxies is strongly decoupled from that of the underlying matter. If, for example, Ly-α emitting galaxies only form at very high density peaks in the underlying mass distribution, they will be far more strongly clustered than matter (eg. Kaiser 1984). Brainerd & Villumsen

(1994) showed that in n-body CDM simulations, dark matter halos cluster far more strongly than the underlying mass at $z \sim 2$. Evidence for such biassing comes from the very different clustering amplitudes inferred for Ly-α forest clouds and metal-line QSO absorption systems (Carswell & Rees 1987, Heisler et al. 1989).

4.2 The Nature of B1

In recent years, a small number of Ly-α emitting galaxies have been found near QSO absorption-line systems (Lowenthal et al. 1991, Møller & Warren 1993, Machetto et al. 1993, Steidel, Sargent & Dickinson 1991). Most are very compact; at best marginally resolved, unlike B1.

The morphology of B1 is however typical of high redshift radio galaxies, which form the vast majority of known high redshift galaxies (McCarthy 1993). B1 resembles these galaxies in many ways: in its elongated irregular morphology, in its Ly-α flux and equivalent width, in its line ratios, in its red continuum colors, and in its red companion objects (Rigler et al. 1992). It lies on the K-band Hubble diagram for powerful radio galaxies. There are however two significant differences: B1's radio flux is at least two orders of magnitude below that of radio galaxies with comparable emission-line fluxes, and the velocity width of Ly-α is about half that of a typical radio galaxy (though this may be due to absorption). Nonetheless, the similarity between B1 and many radio galaxies is striking.

B1 consists of an IR-bright unresolved core (rest-frame absolute V-band magnitude of ~ -24.4), and an extended, asymmetric line-emitting tail (Fig 3). As shown in § 3.2, the core has a pronounced spectral break at $\sim 1.3\mu$m observed-frame, giving it a rest-frame color of $U - V > 1$. Our narrow-band H-α imaging shows that only $< 10\%$ of the K' flux comes from line emission, so we attempted to fit B1's colors using synthetic galaxy spectra from Arimoto & Yoshii (1987), Arimoto, Yoshii & Takahara (1992), Bruzual & Charlot (1993) and Rocca-Volmerange & Guiderdoni (1988). The magnitude of the spectral break can only be reproduced by stellar populations with little ongoing or recent star formation; a population of stars formed in an instantaneous burst and then allowed to passively age for > 0.6 Gyr gives a good fit. If the age is ~ 0.6 Gyr, the 1.3μm break would be due to Balmer absorption in A stars, whose light is expected to dominate galaxies of this age. If older, the break would be the well known 4000Å feature. The stellar mass M derived from the rest-frame V-band light is somewhat model dependent, being somewhere in the range $\sim 2 \times 10^{11}\mathrm{M}_{\mathrm{Sun}} < \mathrm{M} < 2 \times 10^{12}\mathrm{M}_{\mathrm{Sun}}$. Models in which star formation is ongoing or recent predict 0.5μm fluxes significantly above our limits, due to a population of O and B stars. If the tentative detection of continuum flux at 5000 Å in the red spectrum is correct, a small number of blue stars or some non-thermal component would be required. An age of ~ 0.5 Gyr at $z = 2.38$ implies (for $H_0 = 75$km s^{-1}Mpc^{-1}) that formation occurred at $z \sim 3.7$ ($q_o = 0.5$) or $z \sim 3.0$ ($q_0 = 0.1$). If the age were 1Gyr, the epoch of formation would be $z \sim 5$ ($q_0 = 0.5$) or $z \sim 4$ ($q_0 = 0.1$).

What is the cause of the line emission? The Ly-α and H-α flux could be generated by star formation, at a rate of ~ 100 $\mathrm{M}_{\mathrm{Sun}}\mathrm{yr}^{-1}$ (Kennicutt 1983) without overproducing blue continuum light (Charlot & Fall 1993). However the detection of C IV strongly suggests that an AGN is present, as hot stars produce few photons capable of ionizing carbon to this state. The similarity between B1 and radio galaxies also suggests that an AGN is present, albeit a radio-quiet one.

The Ly-α equivalent width of B1 is higher, and the Ly-α line narrower than those of typical QSOs (Francis et al. 1992, Francis 1993). If however the active nucleus were hidden from direct observation by dust clouds, but its radiation could escape in other directions, we would only see scattered light and line emission from photoionized gas far from the nucleus, which might have much higher equivalent widths and lower velocity widths. This is now known to be the explanation of strong narrow lines of many Seyfert 2 galaxies (eg. Antonucci & Miller 1985), and is widely invoked to explain the line emission of radio galaxies.

Many high redshift QSOs and radio galaxies show extended Ly-α emission with fluxes in excess of B1's, originating on scales of up to 100 kpc (eg. Heckman et al. 1991). An AGN with an absolute B magnitude of -23 produces enough ionizing photons to generate the observed Ly-α and H-α fluxes. If the Ly-α flux were produced by photoionization from an AGN concealed in the IR-bright core, the asymmetry of the emission would have to be caused by a highly asymmetric, lumpy gas distribution. Our upper limit on the radio flux of B1 is not inconsistent with the typical radio fluxes of the least radio-loud QSOs (Kellerman et al. 1989).

B1's Ly-α emission peaks ~ 490 km s^{-1} to the red of its C IV emission (Fig 5). We suggest that this offset is caused by Ly-α absorption of the blue part of the Ly-α line. If the absorbing neutral hydrogen is dust-free, it cannot be physically associated with the emission-line region, as it would scatter roughly as many photons into the line of sight as out of it (unless the geometry was very special). If the absorber is indeed a foreground screen of neutral hydrogen, its redshift and column density would have to be similar to those of the central component of the QSO absorption-line. The Ly-α emission would need to be intrinsically red asymmetric, and to have an intrinsic velocity width of ~ 1000 km s^{-1}.

If, alternatively, the absorption occurs in neutral hydrogen mixed with the emission-line gas, dust is needed to absorb the resonantly scattered Ly-α photons. The red wing of Ly-α might escape because the high velocity gas is dust-free, or because the optical depth of the high velocity gas is low.

We conclude that B1 is probably a large early type galaxy, containing a hidden radio-quiet QSO, which is photoionizing the lumpy surrounding gas.

4.3 Evidence for Dust

The observed Ly-α to H-α ratio of B1 is ~ 0.8; well below the case B recombination value of 8. This strongly suggests that dust is present. The Ly-α/H-α ratio is low both in the Ly-α knot and the tail, so the dust must extend over at least 50 kpc.

If all the dust is in a foreground screen, an extinction $E(B-V) \sim 1$ is required to explain the observed ratio. Much smaller amounts of dust will suffice if it is mixed in with the gas, as the optical depth of the gas to resonant scattering of Ly-α is likely to be large, giving the Ly-α photons many chances to be absorbed.

The presence of extended dust in B1, associated with the QSO absorption-line system, supports the contention of Fall & Pei (1993) that high column density Ly-α QSO absorption-line systems contain dust, and therefore can obscure background QSOs. Given the steepness of the QSO luminosity function, even very small quantities of dust in absorption-line systems will seriously bias absorption-line statistics and QSO number counts (eg. Webster et al. 1995).

4.4 The Environment of B1

The region around B1 and the QSO is an extraordinary one. Within a radius of $\sim 10''$ we have three Ly-α absorption components, one Ly-α emitting galaxy and possibly three less active galaxies, C3, C4 and C5. If they are physically associated, they all lie within ~ 100 kpc of each other.

If C3, C4 and C5 really are inactive galaxies at $z = 2.38$, then together with B1 they form a high redshift analogue of a compact group (Hickson, Kindl & Huchra 1989). Many more galaxies could be present but below our detection threshold. The extended irregular emission of B1 suggests that this group of galaxies is embedded in a lumpy cloud of dust and gas.

The absorption in the spectrum of QSO 2139−4434 also suggests the presence of a lumpy gas cloud. It is interesting that the column density of the main QSO absorption component is similar to that needed to absorb the blue wing of B1's Ly-α emission (§ 4.3). If the QSO absorption components really are associated with the gas cloud embedding B1, C3, C4 and C5, we can estimate the mass of this gas cloud: a gas cloud of column density $N_H \sim 10^{19}\mathrm{cm}^{-2}$ and radius 50 kpc will have a neutral hydrogen mass of $\sim 2 \times 10^9 M_{\mathrm{Sun}}$, ie. $\sim 5\%$ of the stellar mass of B1.

On a yet more speculative note, if all three absorption-line components are associated with the galaxy group, we can combine their redshifts with that of B1 to estimate a velocity dispersion for the gas cloud: ~ 500 km s^{-1}. This calculation should be regarded with great caution; quite apart from the small number statistics, the velocities of the three absorption-line components could be dominated by the gravity of a compact galaxy hiding in the point spread function of the QSO. Alternatively, they may lie in different parts of Francis & Hewett's supercluster; if the absorption-line supercluster is roughly spherical and expanding with the Hubble flow, it will have an expected radial extent of ~ 1000 km s^{-1}, greater than the velocity differences between the different absorption-line components. If however 500 km s^{-1} is a reasonable estimate of the velocity dispersion of the group, and this velocity dispersion is dominated by gravitational motions and not by gas dynamics, the virial mass of the group is $\sim 10^{12}\mathrm{M}_{\mathrm{Sun}}$ and the crossing-time is $\sim 10^8$ years.

Irrespective of the velocity dispersion of the group, if B1 and its neighbors are gravitationally bound, their merger timescale will be $\ll 1$ Gyr (but see Governato, Bhatia & Chincarini 1991). We therefore speculate that by redshift zero, B1 will have accreted C3, C4, C5 and much of its gaseous halo, forming a massive elliptical galaxy, perhaps even a cD galaxy.

To summarize, if B1, the color-selected galaxies and the QSO absorption line clouds really are physically associated, they form an extremely gas rich compact group, which may be a giant elliptical galaxy in the act of bottom-up formation.

5 Conclusions

We have detected and confirmed two Ly-α emitting galaxies at $z = 2.38$, associated with a cluster of Ly-α QSO absorption lines. One of these galaxies, B1, lies $22''$ from a background QSO, and is surrounded by a group of very red objects, some of which may be other galaxies at the same redshift. The detection of two Ly-α emitting galaxies in the small area surveyed supports Francis & Hewett's claimed supercluster, though final proof will require the mapping of the rest of the postulated supercluster.

B1 is a massive early-type galaxy, at least 500 Myr old, and probably contains a concealed radio-quiet AGN, which is photoionizing an irregular cloud of gas surrounding B1. Together with its neighboring red galaxies, it may be a giant elliptical galaxy in the act of bottom-up formation.

We have detected H-α emission from B1 at a level indicating that dust is present. This supports Hu et al. (1993) and Bunker et al.'s (1995) contention that H-α searches may be a powerful tool for finding high redshift galaxies. The dust is extended over at least 50 kpc, supporting Fall & Pei's (1993) contention that dust obscuration is important in QSO absorption lines.

The pronounced 1.3μ break in the spectrum of B1 suggests an additional technique for finding high redshift galaxies. With optical and near-IR photometry, it may be possible to select galaxies by the presence of a redshifted Balmer or 4000Å break. The technique is similar to Steidel & Hamilton's (1992) broad-band selection of galaxies showing Ly-limit breaks, but is sensitive to lower redshifts and older galaxies.

We wish to thank Ken Freeman, Dick Hunstead, Bruce Peterson and Rachel Webster for helpful discussions. Dick Hunstead and Taisheng Ye kindly made their Molonglo radio observations available to us. PJF is supported by an ARC grant, and acknowledges travel support from ANSTO.

Candidate	Coordinates (B1950)	Ly-α Flux (erg cm^{-2}s^{-1})	Ly-α Equivalent Width (3σ, Å observed-frame)
B1	21:39:16.32 - 44:34:12.9	$8 \pm 1 \times 10^{-16}$	> 270
B2	21:39:18.50 - 44:34:44.9	$3 \pm 0.3 \times 10^{-16}$	> 160
B3	21:39:16.82 - 44:34:40.7	$0.8 \pm 0.3 \times 10^{-16}$	—
2139-4434	21:39:14.62 - 44:34:00.5	—	

MM acknowledges the support of a University of Melbourne Fellowship for Women with Career Interruptions. AJB acknowledges a UK Particle Physics and Astronomy Research Council studentship. YY acknowledges financial support of the Yamada Science Foundation for transport of the PICNIC camera and IR team. Astrometry was done using coordinates from the COSMOS database, maintained on-line by the AAO.

6 References

Arimoto, N., & Yoshii, Y. 1987, A & A, 173, 23

Arimoto, N., Yoshii, Y., & Takahara, F. 1992, A & A, 253, 21

Antonucci, R. R. J., & Miller, J. S. 1985, ApJ, 297, 621

Baron, E., & White, S. D. M. 1987, ApJ, 322, 585

Brainerd, T. G., & Villumsen, J. V. 1994, ApJ, 431, 477

Bruzual A. G., & Charlot, S. 1993 ApJ, 405, 538

Bunker, A. J., Warren, S. J., Hewett, P. C., & Clements, D. L. 1995, MNRAS, 273, 513

Butcher, H., & Oemler, A. 1978 ApJ, 219, 18

Carswell, R. F., & Rees, M. J. 1987, MNRAS, 224, 13p

Colless, M., Ellis, R. S., Taylor, K., & Hook, R. N. 1990, MNRAS, 244, 408

Charlot, A., & Fall, S. M. 1993, in First Light in the Universe, Stars or QSOs? ed. B. Rocca-Volmeragne et al. (Gif-sur-Yvette: Editions Frontiéres), 341

De Propris, R., Pritchet, C. J., Hartwick, F. D. A., & Hickson, P. 1993, AJ, 105, 1243

Dekker, H., D'Odorico, S., Kotzlowski, K., Lizon, J.-L., Longinotti, A., Nees, W., & De Lapparent-Gurriet, V. 1991, ESO messenger, 63, 73

Djorgovski, S., Spinrad, H., McCarthy, P., & Strauss, M. A. 1985, ApJl, 299, L1

Djorgovski, S., Thompson, D., & Smith, J. D. 1993, in First Light in the Universe, Stars or QSOs? ed. B. Rocca-Volmerange et al. (Gif-sur-Yvette: Editions Frontiéres), 67

Dressler, A., Oemler, A., Gunn, J. E., & Butcher, H. 1993, ApJl, 404, L45

Eckert, W., Hofstadt, D., & Melnick, J. 1989, ESO messenger, 57, 66

Edge, A. C., Stewart, G. C., Fabian, A. C., & Arnaud, K. A. 1990, MNRAS, 245, 559

Efstathiou, G., Bernstein, G., Katz, N., Tyson, J. A., & Guhathakurta, P. 1991, ApJl, 380, L47

Evrard, A. E., & Charlot, S. 1994, ApJl , 424, L13

Foltz, C. B., Hewett, P. C., Chaffee, F. H., & Hogan, C. J. 1993, AJ, 105, 22

Fall, S. M., & Pei, Y. C. 1993, ApJ, 402, 479

Francis, P. J. 1993, ApJ, 405, 119

Francis, P. J., & Hewett, P. C. 1993, AJ, 105, 1633

Francis, P. J., Hewett, P. C., Foltz, C. B., & Chaffee, F. H., 1992, ApJ, 398, 476

Gebhardt, K., Pryor, C., Williams, T. B., & Hesser, J. E. 1994, AJ, 107, 2067

Giavalisco, M., Steidel, C. C., & Szalay, A. S. 1994, ApJl, 425, L5

Glazebrook, K., Ellis, R., Colless, M., Allington-Smith, J., & Tanvir, N. 1995, MNRAS, 273, 157

Governato, F., Bhatia, P., & Chincarini, G. 1991, ApJl, 371, L15

Heckman, T. M., Lehnert, M. D., van Breugel, W., & Miley, G. K. 1991, ApJ, 370, 78

Heisler, J., Hogan, C. J., & White, S. D. M. 1989, ApJ, 347, 52

Hickson, P., Kindl, E., & Huchra, J. P., 1989, ApJ, 331, 64

Hu, E. M., Songaila, A., Cowie, L. L., & Hodepp, K. -W. 1993, ApJl, 419, L13

Jakobsen, P., & Perryman, M. 1992, ApJ, 392, 432

Kaiser, N. 1984, ApJl, 284, L9

Kellerman, K., Sramek, R., Schmidt, M., Shaffer, D., & Green, R. 1989, AJ, 98, 1195

Kennicutt, R. C. 1983, ApJ, 272, 54

Kobayashi, Y., Fang, G., Minezaki, T., Waseda, K., & Nakamura, K. 1994 in SPIE proceedings "Instrumentation in Astronomy 8", 2198, 603

Leggett, S. K. 1992, ApJs, 82, 351

Lowenthal, J. D., Hogan, C. J., Green, R. F., Caulet, A., Woodgate, B. E., Brown, L., & Foltz, C. B. 1991, ApJl, 377, L73

Lowenthal, J. D., Hogan, C. J., Green, R. F., Woodgate, B. E., Caulet, A., Brown, L., & Bechtold, J. 1995, ApJ, in press

Machetto, F., Lipari, S., Giavalisco, M., Turnshek, D. A., & Sparkes, W. B. 1993, ApJ, 404, 511

McCarthy, P. J. 1993, Ann Rev Ast. Ast., 31, 639

Møller, P., 1995, A & A, in press

Møller, P., & Warren, S. J., 1993, A & A, 270, 43

Pritchet, C. J., & Hartwick, F. D. A. 1990, ApJl, 355, L11

Rees, M. J. 1988, MNRAS, 231, 91p

Rigler, M. A., Lilly, S. J., Stockton, A., Hammer, F., & LeFèvre, O., 1992, ApJ, 385, 61

Rocca-Volmerange, B., & Guiderdoni, B. 1988, A & A Supp, 75, 93

Rodrigues-Williams, L. L., & Hogan, C. J. 1994, AJ, 107, 451

Steidel, C. C., & Hamilton, D. 1992, AJ, 104, 941

Steidel, C. C., Sargent, W. L. W., & Dickinson, M. 1991, AJ, 101, 1187

Webster, R. L., Hewett, P. C., Harding, M. E., & Wegner, G. A. 1988, Nature, 336, 358

Webster, R. L., Francis, P. J., Peterson, B. A., Drinkwater, M. J., & Masci, F. J. 1995, Nature, 375, 469

Williger, G. M., Hazard, C., Baldwin, J. A., & McMahon, R. G. 1995 ApJ, submitted

Wolfe, A. M. 1993, ApJ, 402, 411

Figure 1: Ly-α On-band (left) and off-band (right) images of the field around QSO 2139-4434. Images have been lightly smoothed by a Gaussian of $\sigma = 0.6''$, axes are in B1950 coordinates. See Fig 2 for the names of the objects.

Figure 2: Identification chart for the images. The orientation and field of view of this chart is the same as that of figures 1 and 6. Solid triangles are Ly-α emission candidates; squares are objects with large $I - K'$ colors; ie. candidate cluster members (§ 3.2). Circles are objects red in $B - K'$ but not in $I - K'$; ie. candidate foreground galaxies. Other objects are marked with crosses and are probably foreground stars and galaxies.

Figure 3: Close-up of B1. The K' image is shown in greyscales, and the narrow-band Ly-α image (smoothed with a Gaussian beam of $\sigma = 0.56''$) is shown by contours. Contours are equally spaced; the zero level contour is dotted. The internal astrometry of the K' and Ly-α images is good to $\sim 0.15''$, based on the rms fit of the positions of all the images; the misalignment of the object in the top right is also real.

Figure 4: NTT Spectra of B1 and B2 and the QSO 2139$-$4434, showing the Ly-α lines. A higher resolution spectrum of the QSO can be found in Francis & Hewett (1993).

Figure 5: C IV and Ly-α emission from B1 (NTT spectra). The Ly-α absorption line in the spectrum of QSO 2139$-$4434 is shown for comparison.

Figure 6: I-band and Siding Spring 2.3-m K'-band (right) images. The white patches above and below the brightest sources are artifacts of the data reduction.

Figure 7: Spectral energy distributions for a number of candidate galaxies. The distributions marked (a) are for two representative red objects showing a break between B and I; ie. candidate foreground galaxies. The different objects have displaced vertical scales for clarity. The data points are for standard B, I, J, H and K' bands except for B1, where a more stringent limit on the blue flux is placed at 5000Å from our spectra.

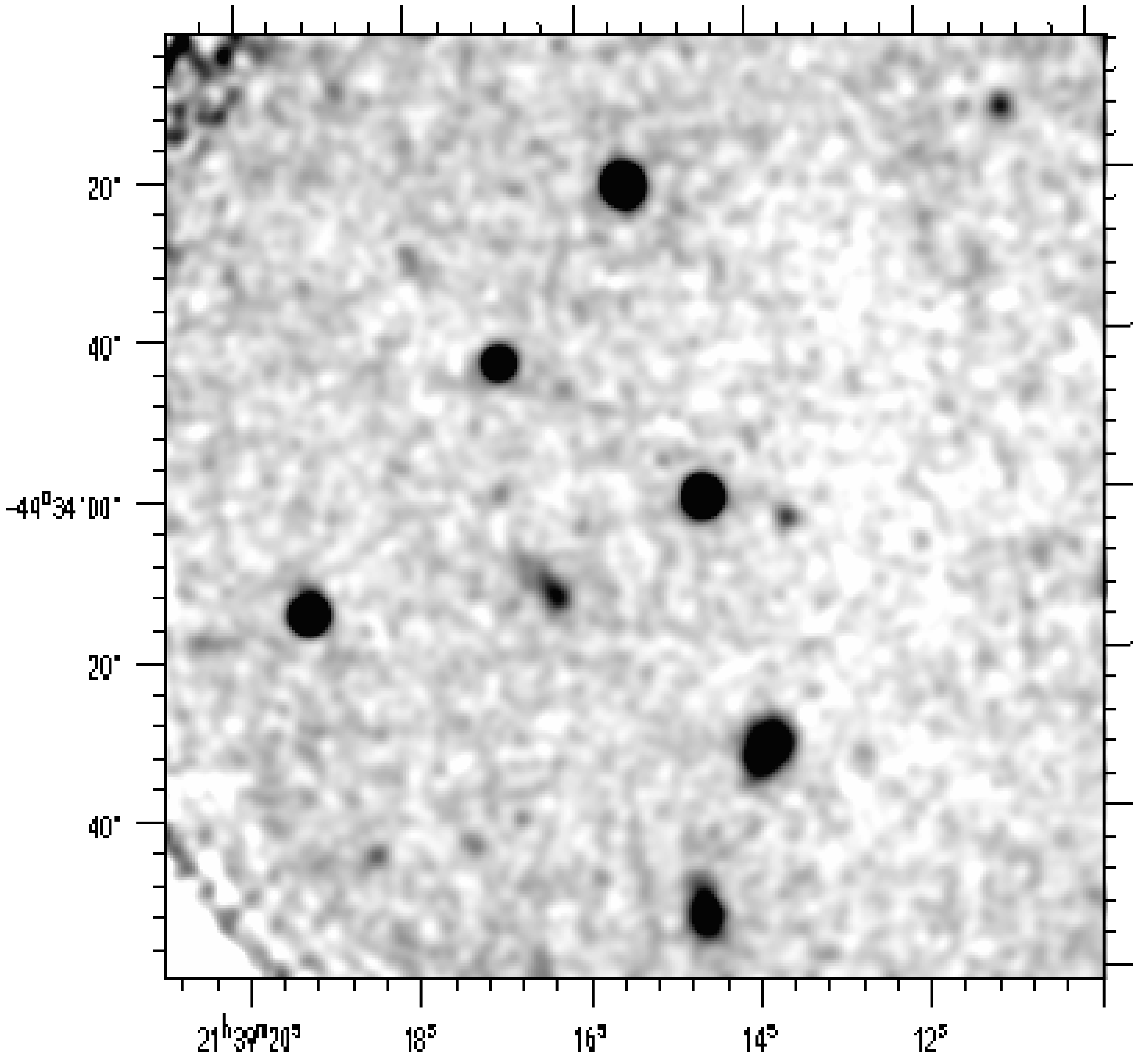
20"
40"
−44°34'00"
20"
40"
21h39m20s
18s
16s
14s
12s

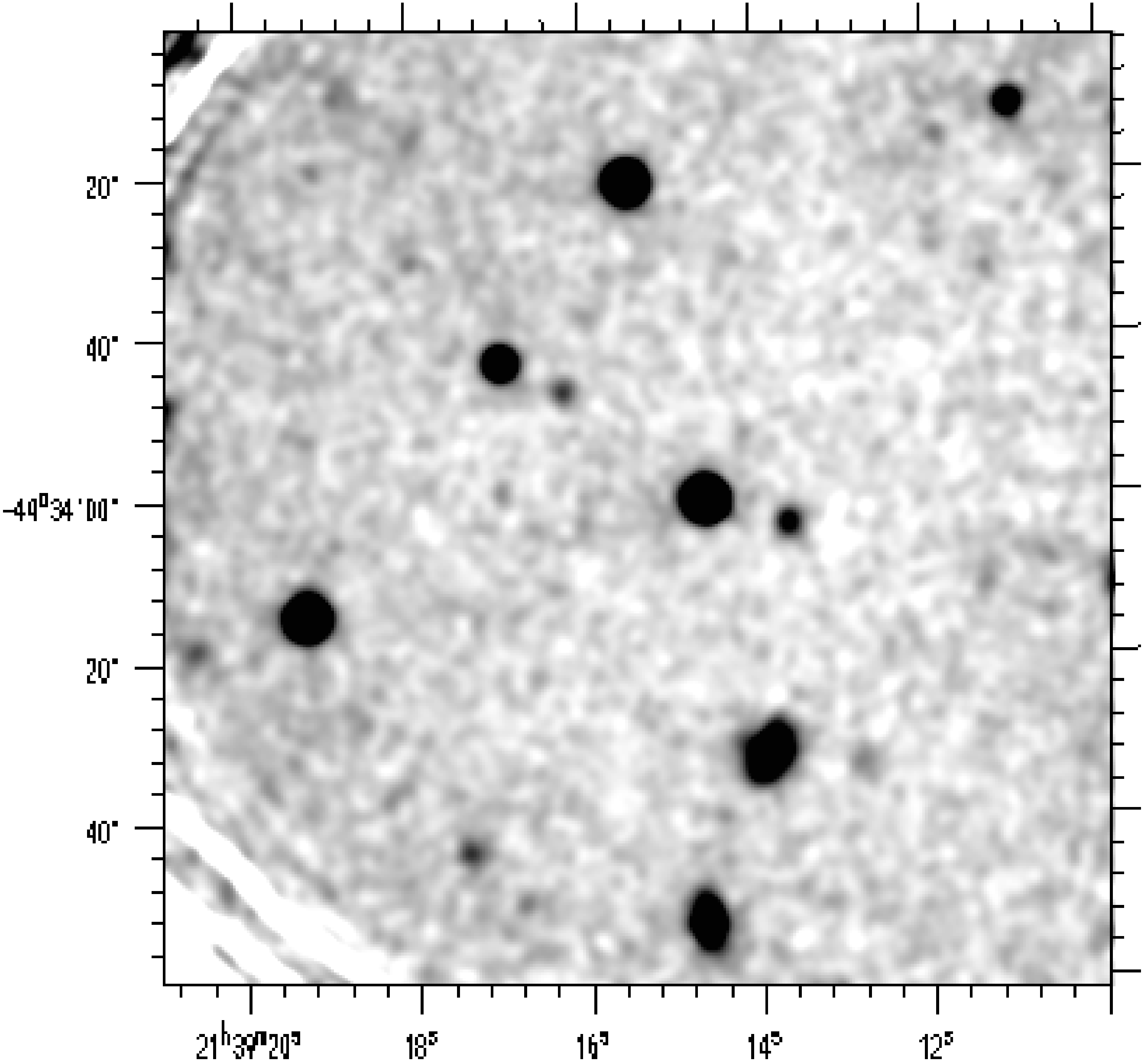
20"
40"
-44°34'00"
20"
40"
21h39m20s
18s
16s
14s
12s

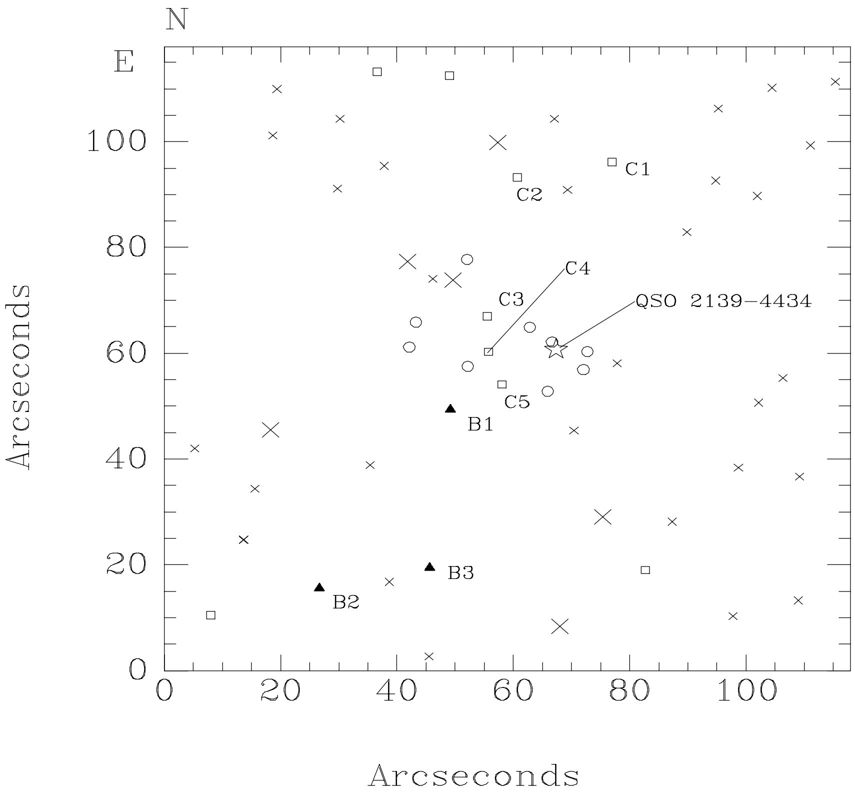
N
E
C1
C2
C3
C4
C5
QSO 2139-4434
B1
B2
B3
Arcseconds
Arcseconds
0
20
40
60
80
100

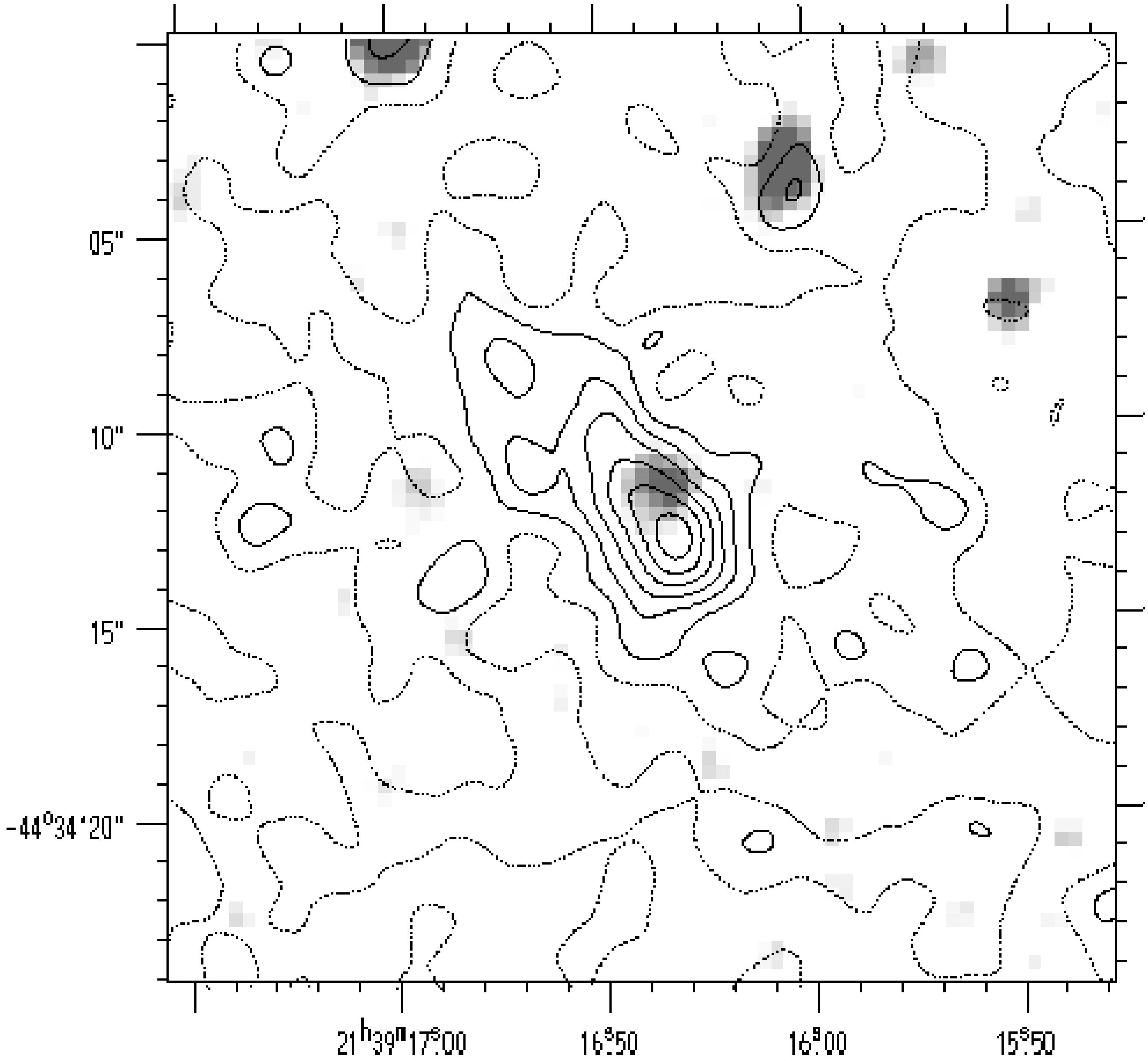
05"
10"
15"
-44°34'20"
21h39m17s.00
16s.50
16s.00
15s.50

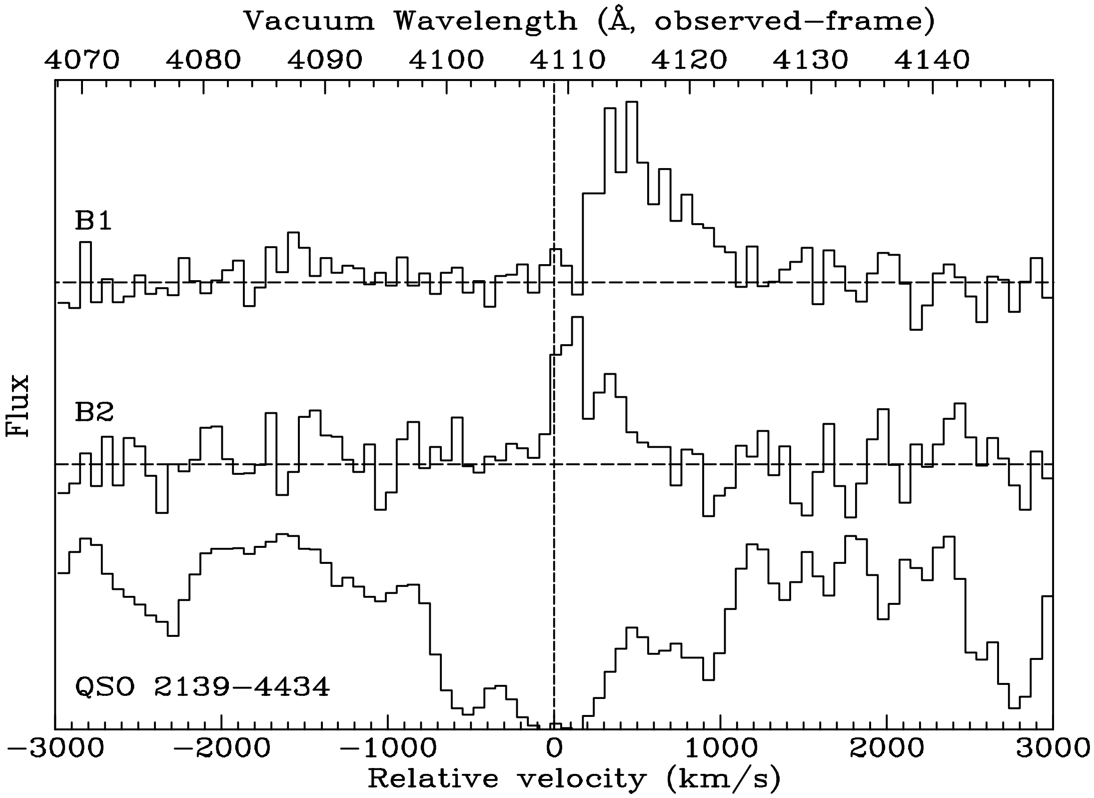
Vacuum Wavelength (Å, observed−frame)
4070
4080
4090
4100
4110
4120
4130
4140
B1
B2
QSO 2139−4434
Flux
−3000
−2000
−1000
0
1000
2000
3000
Relative velocity (km/s)

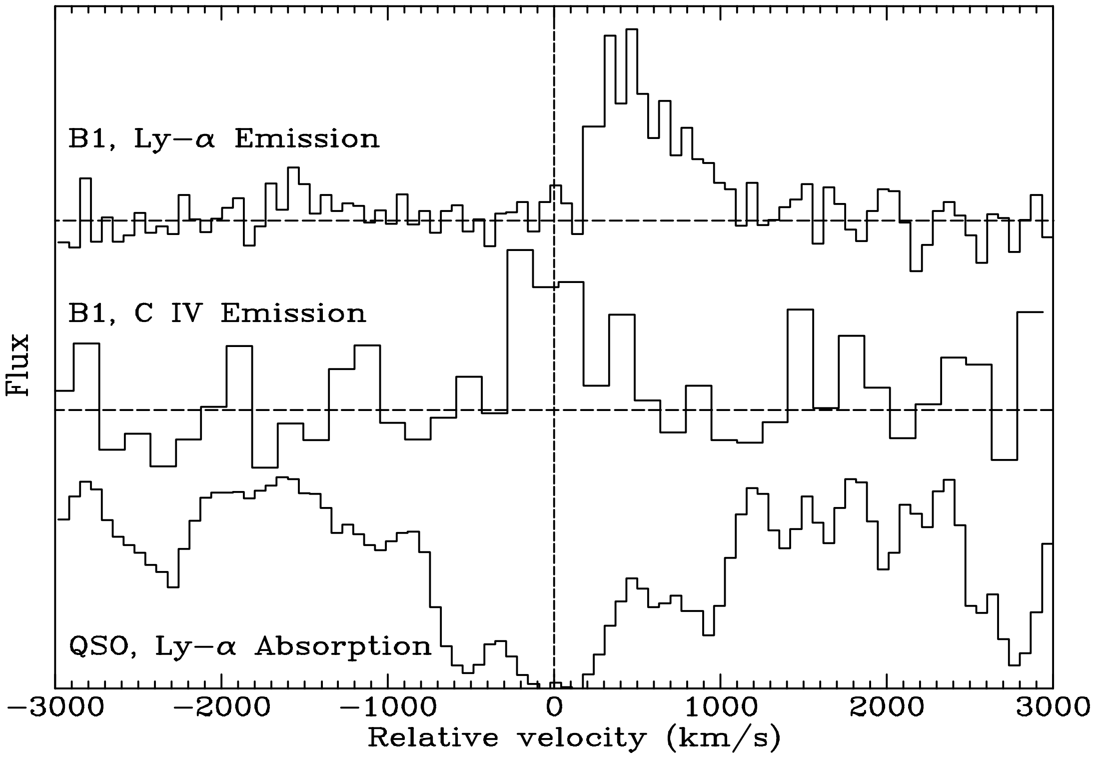
B1, Ly$-\alpha$ Emission
B1, C IV Emission
QSO, Ly$-\alpha$ Absorption
Flux
−3000
−2000
−1000
0
1000
2000
3000
Relative velocity (km/s)

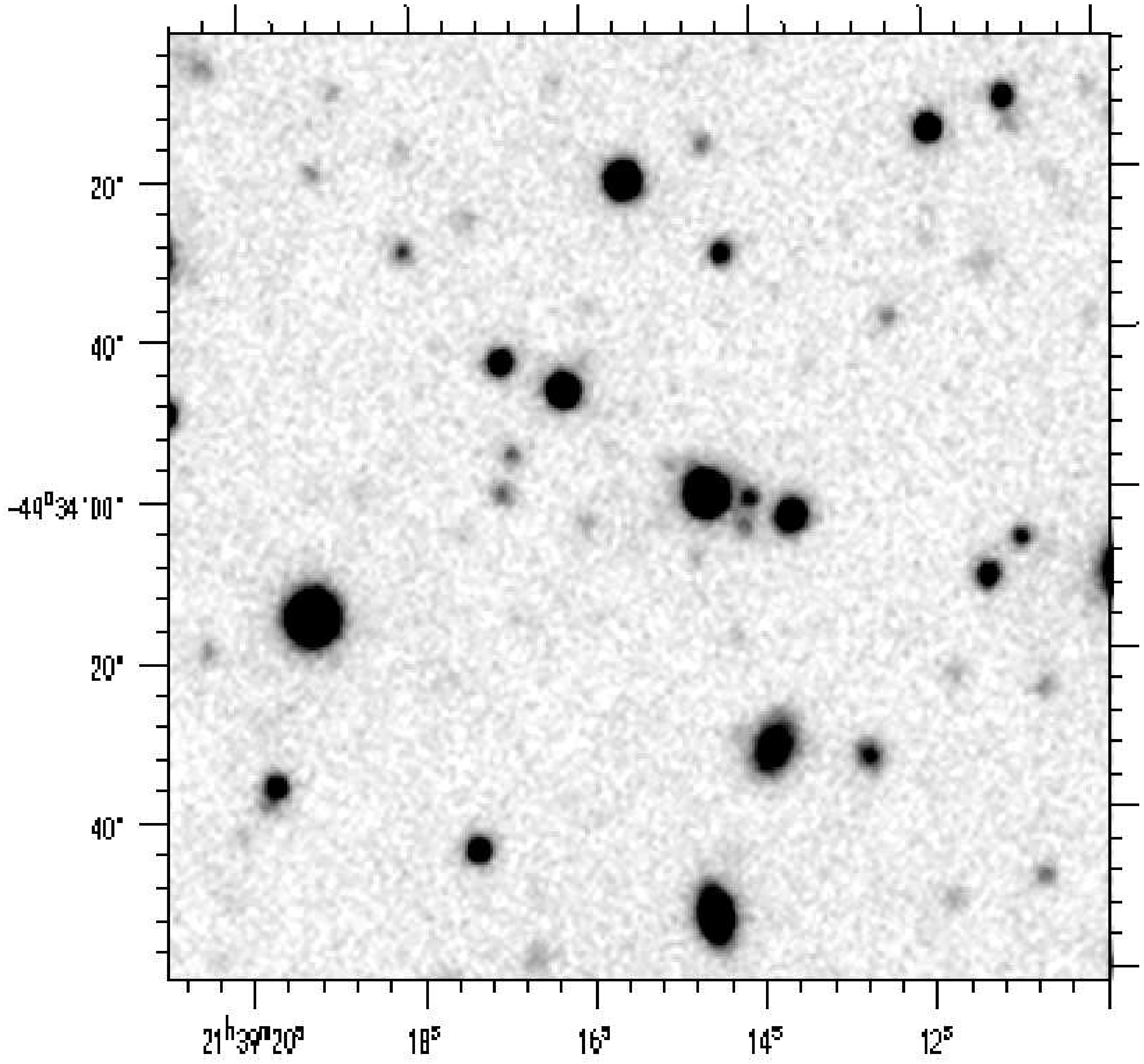
20"
40"
-44°34'00"
20"
40"
21h37m20s
18s
16s
14s
12s

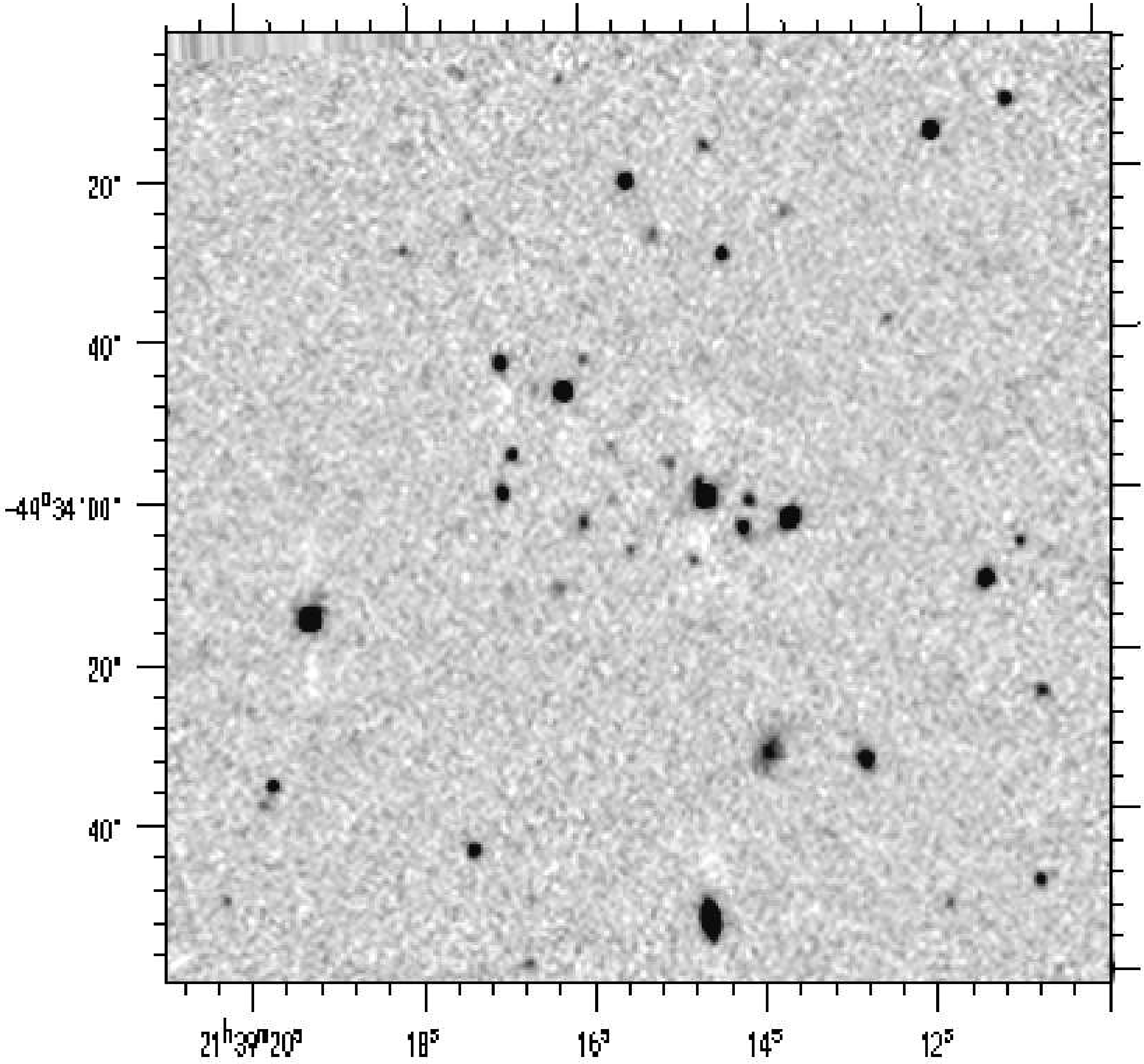
20"
40"
-49°34'00"
20"
40"
21h39m20s
18s
16s
14s
12s

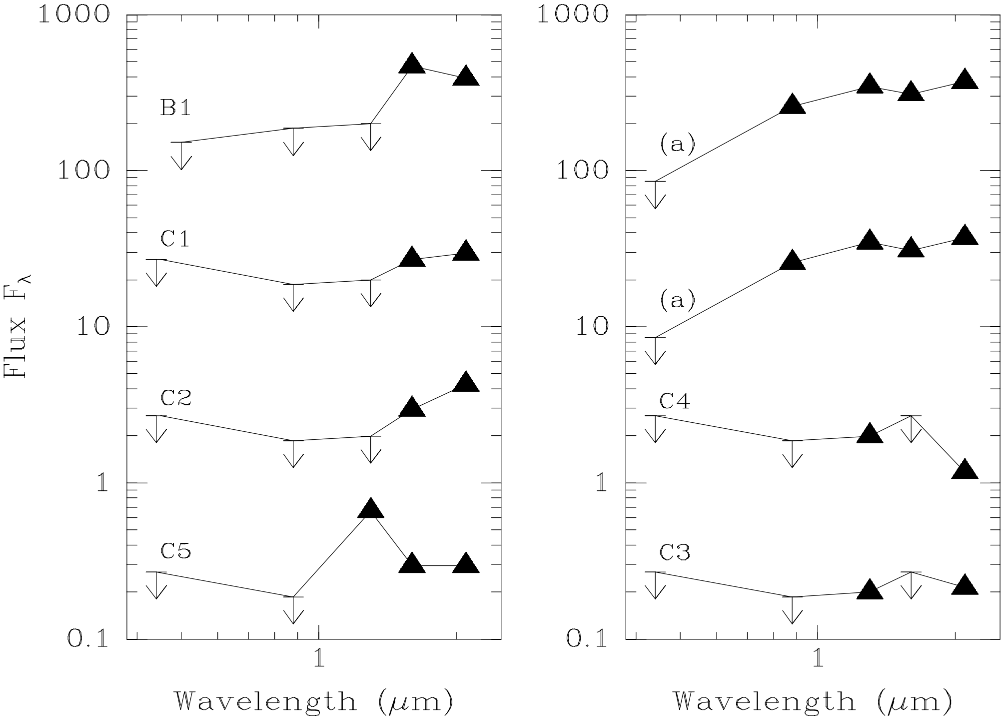

1000
100
10
1
0.1
Flux F_λ
B1
C1
C2
C5
1
Wavelength (μm)
1000
100
10
1
0.1
(a)
(a)
C4
C3
1
Wavelength (μm)